

PantaRei VII, il Minoico ed il Disco di Festo

Original

PantaRei VII, il Minoico ed il Disco di Festo / Sparavigna, A.C.. - ELETTRONICO. - (2026). [10.5281/zenodo.19334091]

Availability:

This version is available at: 11583/3009378 since: 2026-03-30T12:14:23Z

Publisher:

Published

DOI:10.5281/zenodo.19334091

Terms of use:

This article is made available under terms and conditions as specified in the corresponding bibliographic description in the repository

Publisher copyright

(Article begins on next page)

PAPER • OPEN ACCESS

Development of a Flight Mechanics Simulation Computer based on a Flexible Aircraft Model for a Regional Aircraft

To cite this article: Simone Malisani *et al* 2021 *IOP Conf. Ser.: Mater. Sci. Eng.* **1024** 012066

View the [article online](#) for updates and enhancements.

The 17th International Symposium on Solid Oxide Fuel Cells (SOFC-XVII)
DIGITAL MEETING • July 18-23, 2021

EXTENDED Abstract Submission Deadline: February 19, 2021



SUBMIT NOW →

Development of a Flight Mechanics Simulation Computer based on a Flexible Aircraft Model for a Regional Aircraft

Simone Malisani¹, Elisa Capello² and Giorgio Guglieri³

¹Graduate Research Fellow, Department of Mechanical and Aerospace Engineering, Politecnico di Torino, Corso Duca degli Abruzzi 24, Torino, 10129, Italy

²Assistant Professor, Department of Mechanical and Aerospace Engineering, Politecnico di Torino, CNR-IEIIT, Corso Duca degli Abruzzi 24, Torino, 10129, Italy

³Professor, Department of Mechanical and Aerospace Engineering, Politecnico di Torino, Corso Duca degli Abruzzi 24, Torino, 10129, Italy

E-mail: simone.malisani@polito.it

Abstract. The changes on aircraft structures and the increased use of advanced and light materials have led to the design of more efficient and flexible aircraft. This implies that rigid body dynamics is no longer sufficient to describe the aircraft behaviour in atmospheric flight. Coupling between structural and rigid body dynamics should be included, due to frequencies of structural modes. In this work, an analytical method, based on a mixed Newtonian-Lagrangian approach, is used to derive a simplified model of a flexible aircraft. Moreover, flexible displacements and torsional variables, starting from the Lagrange's equations, are discretized by means of a finite number of generalized coordinates. This approach allows to derive directly a finite-order system of ordinary differential equations, making it less complex and suitable for real time simulation and control law synthesis. The main objective of the proposed methodology is the real-time implementation on a "flyable" hardware, for experimental tests, including sensor models. In detail, accelerometers on selected wing sections are design to measure the effect of flexibility in terms of bending and torsional deformations. A simplified low-order model is designed for a regional aircraft, including different masses and flight conditions. Moreover, only two symmetrical bending modes and one torsional mode are considered in the flexibility definition. Finally, the hinge moments acting on the control surfaces are evaluated. The hinge moment is calculated as the aerodynamic torque generated on the hinge axis by the variation of the pressure distribution acting on the control surfaces. A gust response of this aircraft is mainly analysed, considering both a discrete gust model and a continuous model. This research is performed within the ASTIB project, which has received funding from the Clean Sky 2 Joint Undertaking under the European Union's Horizon 2020 research and innovation program under grant agreement CSJU – GAM REG 2014-2015.

1. Introduction

Due to progress in aerospace materials and on optimised structural design, more light and slender aircraft structures are designed, to obtain weight, drag reduction and, consequently, more efficient aircraft in terms of fuel consumption. However, these slender structures tend to be highly deformable, and thus the assumption of rigid body is no longer acceptable [1]. Moreover, the deformation of the structure increases fatigue loads by means of dynamic loads



Content from this work may be used under the terms of the [Creative Commons Attribution 3.0 licence](https://creativecommons.org/licenses/by/3.0/). Any further distribution of this work must maintain attribution to the author(s) and the title of the work, journal citation and DOI.

generated by maneuvers and/or by external perturbations. Finally, more flexibility leads to lower frequencies of the structural modes which might couple with typical aircraft dynamics frequencies [2] resulting in dangerous resonance phenomenons.

Comprehensive mathematical formulations of the problem have been derived for both structural dynamics [3] and aeroelastic [4] purposes, since many years. Nevertheless, these formulations are usually not suitable for real-time applications because of their high complexity level. For this reason, in early 1960s, strong simplifications were required to find equations solutions, because of the lack of computational power. The work of Milne [5] is an example, in which small deformations were considered for the aircraft longitudinal motion.

In 2004, Meirovitch and Tuzcu [6] presented a Lagrangian-based model, avoiding the use of some reference frames. Their approach consists in deriving an hybrid system of ordinary and partial differential equations in terms of quasi-coordinates (or generalized coordinates), which permits to express the transport degrees of freedom in terms of flight variables, as linear and angular velocities. This is convenient for real time simulation of the flexible structure but compromises the simplicity of the formulation, since the Lagrange's equation has to take in consideration additional terms and, also, the obtained hybrid system of ordinary and partial equations needs some form of discretization.

Avanzini *et.al.* [7] proposed a minimum-complexity flexible model, which includes the effects of bending and torsion of fuselage and wing on the aircraft rigid dynamics. In [7] classical equations of flight dynamics are derived the rigid degrees of freedom and the Lagrange's equations are considered for the flexible terms.

The method proposed in our paper is based on [7], even if only the wing is considered as deformable system. The main objectives of this approach are: (i) definition of a low order model for wing dynamic loads, including flexible effects, and (ii) a computational efficient algorithm, combined with a control system synthesise, to improve the overall flight dynamics. Even if this modeling framework introduces some simplifications, it is particularly convenient for real time simulations and for the design of control laws, with interactions between structure dynamics, flight mechanics and control.

In particular, this modeling framework is used for the definition of Flight Mechanics Simulator Computer (FMSC), which includes the wing deformation caused by an external perturbation. The objective of the FMSC is to provide real-time aircraft simulation, in order to test equipment behavior in a controlled environment. For this reason, the FMSC does not only include the aircraft rigid and flexible dynamics models, but also gust models to perturb the aircraft and sensor models, such as accelerometers on different wing sections to evaluate the aircraft response. Moreover, also the hinge moments of the control surfaces are evaluated. This work includes two different gust models: (1) a discrete gust model, with a "1-cos" shape, implemented following CS-25 regulations, and (2) a continuous gust model based on von Karman theory, as described in [8, 9]. The first is easy to implement and to simulate large deformations, while the second is more realistic and effective to excite the flexible modes of the wing. Both gust models are used to derive a gust velocity time history which is used as a perturbation inside the aircraft equations of motion. In the CS2 framework, the FMSC system is used for rig experimental tests, computationally efficient and able to handle not only pilot inputs and trim positions, but also gust disturbances.

The paper is organized as follows. In Section 2 an overview of the simulation system is provided, with description of rigid and flexible dynamics. In the same section, accelerometers, gust models and evaluation of the hinge moments are also included. The results are presented in Section 3. Finally, some concluding remarks are described in Section 4.

2. Flight Mechanics Simulation Computer Overview

The FMSC primary role is to provide real-time aircraft simulation, in order to verify the equipment behavior in a simulated real-time environment. The simulator is developed in Matlab/Simulink environment and all subsystems are verified using a fixed-step integrator (Runge-Kutta) with a sample frequency of 100 Hz, considering real equipment hardware. A gust disturbance and a variation of the control surfaces are considered as inputs. The outputs of the FMSC are rigid and flexible variables (due to the presence of wing accelerometers) and the hinge moments of the control surfaces.

As in Figure 1, trim conditions (pilot inputs) and deflections of the control surfaces are input of the system dynamics, with the gust disturbance. In the output section, hinge moments and sensor models (in particular, accelerations on selected wing sections) are the outputs of this system, since an open-loop FMSC scheme is analyzed. The design of control laws is not considered in this paper.

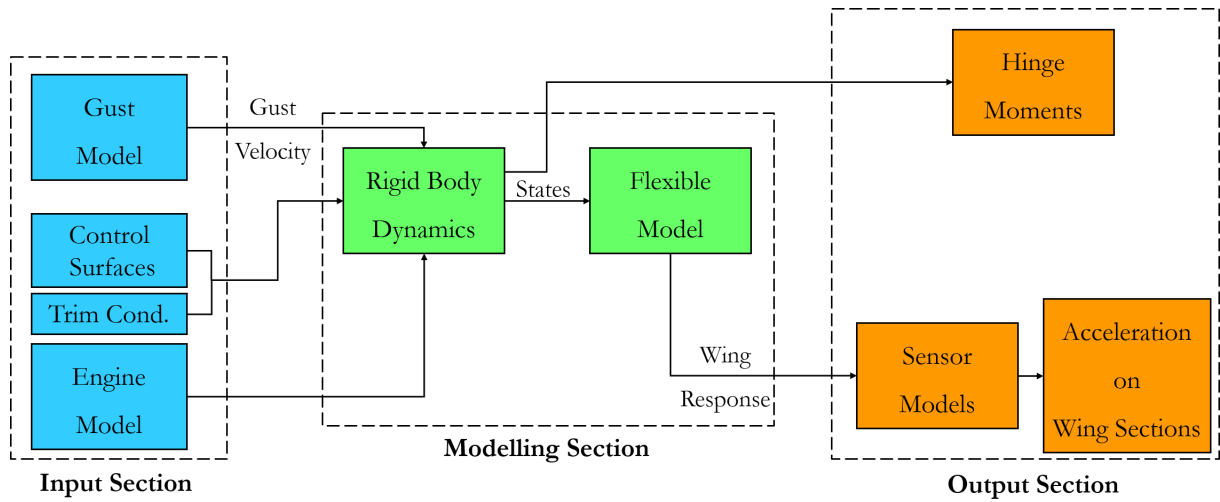


Figure 1. FMSC Open-loop Scheme

2.1. Rigid Aircraft Dynamics

The rigid model is based on nonlinear equations of motion, written in body frame as in [10]. The resulting 6 Degree-of-Freedom (DoF) differential equation system includes 12 variables: linear velocities $U = [u, v, w]^T \in \mathbb{R}^3$, angular rates $\omega = [p, q, r]^T \in \mathbb{R}^3$, Euler angles $\Phi = [\phi, \theta, \psi]^T \in \mathbb{R}^3$ (order of rotation: 3-2-1) and, finally, linear positions $X = [x_N, y_E, z_D]^T \in \mathbb{R}^3$ in North-East-Down (NED) reference frame.

As well known, force equations are classically expressed directly in terms of linear accelerations, as reported in the following matrix form

$$\dot{U}_B = -\tilde{\omega}_B \times U_B + \frac{g}{W} F_B, \quad (1)$$

where F_B represents the aerodynamic forces along the body axes, $\tilde{\omega}_B$ is the skew symmetric matrix, g is the the gravitational acceleration and W is the aircraft weight. In a similar way, moment equations are expressed as follows

$$\dot{\omega}_B = [I_B]^{-1} (M_B - \tilde{\omega}_B [I_B] \omega_B), \quad (2)$$

in which M_B represents the aerodynamic moments vector in body reference frame and $I_B \in \mathbb{R}^{(3,3)}$ is the tensor of inertia.

The Euler angles are defined starting from the kinematic equations

$$\dot{\Phi} = \begin{bmatrix} 1 & \frac{S_\phi \cdot S_\theta}{C_\theta} & \frac{C_\phi \cdot S_\theta}{C_\theta} \\ 0 & C_\phi & -S_\phi \\ 0 & \frac{S_\phi}{C_\theta} & \frac{C_\phi}{C_\theta} \end{bmatrix} \omega_B, \quad (3)$$

where $S_{(\cdot)}$ and $C_{(\cdot)}$ are respectively sine and cosine functions.

Finally, position coordinates in NED reference frame are defined by means of navigation equations

$$\dot{X}_{NED} = L_{EB} U_B, \quad (4)$$

where L_{EB} is the matrix of direction cosines, between NED and body reference frames.

2.2. Flexible Model

The flexible model is based on a Lagrangian approach and considers the wing as a deformable element, while the rest of the aircraft is considered rigid. In order to represent the behavior of a flexible system reducing the model complexity, an appropriate set of generalized coordinates must be chosen. The Gal rkin method [11] is used to define the wing bending and torsional modes as truncated series expansions, in the form

$$\xi_w(x_w, t) = \sum_{j=1}^N \Phi_j(x_w) \eta_j^w(t), \quad (5) \quad \theta_w(x_w, t) = \sum_{j=1}^N \Psi_j(x_w) \zeta_j^w(t), \quad (6)$$

where $\eta_j^w(t)$ and $\zeta_j^w(t)$ are the amplitudes of the structural modes represented by $\Phi_j(x_w)$ and $\Psi_j(x_w)$ shape functions, which should satisfy the physical and geometric boundary conditions of the considered element. The number of structural modes influences the required computational effort.

In this study, we design the flexible model only for the longitudinal motion, so only the symmetric aeroelastic modes affect the aircraft responses. In detail, only the first two symmetric bending modes and the first symmetric torsional mode are considered. According to Eq. (5), wing bending and torsional displacements can be expressed as

$$\xi_w(x_w, t) = \Phi_1(x_w) \eta_1^w(t) + \Phi_2(x_w) \eta_2^w(t), \quad (7) \quad \theta_w(x_w, t) = \Psi_1(x_w) \zeta_1^w(t). \quad (8)$$

In this way, the elastic displacements are represented by means of a finite number of generalized coordinates, represented by the bending and torsional modes amplitudes $\eta = [\eta_1, \eta_2, \zeta_1]^T \in \mathbb{R}^3$. Therefore, the complete state vector of the aeroelastic system can be expressed as $\mathbf{x} = [\mathbf{U}, \omega, \Phi, \mathbf{X}, \eta]^T \in \mathbb{R}^{15}$.

Once the appropriate set of coordinates is chosen, the flexible dynamics is derived by means of Lagrange equations,

$$\frac{d}{dt} \frac{\partial \mathcal{L}}{\partial \dot{q}} - \frac{\partial \mathcal{L}}{\partial q} = Q_q, \quad (9)$$

with q generalized coordinates. Q_q represents the generalized forces and \mathcal{L} is the Lagrangian, defined as

$$\mathcal{L} = \mathcal{T} - \mathcal{U}, \quad (10)$$

with \mathcal{T} and \mathcal{U} kinetic and potential energies, respectively. The kinetic energy is expressed as sum of the energy generated by the linear velocity and the energy generated by the angular

velocity of the wing elements. The potential energy can be considered as sum of the energy generated by the wing bending, calculated using the Euler-Bernoulli beam theory, and the wing torsion.

The generalized forces Q_q can be defined through the principle of virtual work $\partial W = \sum_{h=1}^k F_h \cdot \partial r_h$, where, for the variable r in presence of k external forces, ∂r is the virtual displacement which could be also expressed in terms of the N generalized coordinates. So, in general, the generalized forces can be expressed as

$$Q_{q_j} = \sum_{h=1}^k F_h \frac{\partial r_h}{\partial q_j} \quad \text{with } j = 1, \dots, N. \quad (11)$$

In this study, the virtual work of each flexible part can be expressed as a function of external forces that act on it (i.e., aerodynamic distributed and concentrated loads) multiplied by the virtual displacements, which are the dependent variables. In this work, the aerodynamic force and moment of each wing sections are considered to be function only on the longitudinal angle of attack, due to maneuvers and wing deformations, as in [7],

$$f_{Aw} = \frac{1}{2} \rho V^2 S C_{L\alpha} \alpha_w, \quad (12) \quad M_{Aw} = \frac{1}{2} \rho V^2 S C_{L\alpha} (x_\theta - x_{CA}) \alpha_w, \quad (13)$$

where $(x_\theta - x_{CA})$ represents the distance between the torsional axis and the airfoil aerodynamic center, and α_w is given by the sum of aircraft angle of attack α_{WB} , wing twist angle i_w , pitch rate q , bending rate $\dot{\xi}$, torsion angle θ and its time derivative $\dot{\theta}$. As follows,

$$\alpha_w \approx \alpha_{WB} + i_w(x_w) - \frac{q}{u} x_F(x_w) + \frac{\dot{\xi}_w(x_w, t)}{u} + \theta_w(x_w, t) + \frac{\dot{\theta}_w(x_w, t)(x_\theta - x_{CA})}{u}, \quad (14)$$

where x_F represents the distance between the aerodynamic center of the considered section and the aircraft center of gravity in body reference frame.

External aerodynamic force and moment can be written as in [7]

$$f_{Aw}(x) = f_{A_0} + \frac{\partial f_A}{\partial \dot{\xi}_w} \dot{\xi}_w \quad (15) \quad M_{Aw}(x) = M_{A_0} + \frac{\partial M_A}{\partial \dot{\theta}_w} \dot{\theta}_w, \quad (16)$$

where the subscript 0 indicates the aerodynamic load generated by the "frozen" configuration and the second term is the increment generated by deformation rates. This approach permits to split the virtual work, expressed for the k -th wing element as discussed in [7].

While the derivation of the first term is straightforward, the second term of Eq. (15) and (16), generated by deformation rates, can be expressed in terms of Rayleigh dissipation function \mathcal{F} as deeply discussed in [3, 6, 7]. The Rayleigh dissipation function is used to represent the viscous damping forces by means of a single scalar. The viscous damping is proportional to the generalized velocities \dot{q}_j and is one of the most important non-conservative forces acting on an aerodynamic surface. Starting from this definition of the external forces, the Lagrange equation could be written as

$$\frac{d}{dt} \frac{\partial \mathcal{L}}{\partial \dot{q}} - \frac{\partial \mathcal{L}}{\partial q} + \frac{\partial \mathcal{F}}{\partial \dot{q}} = Q_{q_0}, \quad (17)$$

where Q_{q_0} represents the generalized forces generated by the "frozen" configuration. In this work, when referring to the generalized forces Q_q both "frozen" and viscous damping forces are considered.

Since we are considering only two bending modes and one torsional mode, the complete system can be written as three Lagrange equations, one for each of the considered structural modes. Reorganizing the system in matrix form, a second order mass-spring-damper system (MCK) is obtained

$$M\ddot{q} + C\dot{q} + Kq = f_q. \quad (18)$$

2.3. Gust Models

As stated before, both discrete and continuous gust models are defined as aircraft perturbation. In both considered model, a gust velocity profile is added to the linear speed components.

The discrete gust model, as in CS 25 regulation [12], consists in a "1 – cos" pulse

$$U_g = \begin{cases} \frac{U_{ds}}{2} \left[1 - \cos\left(\frac{\pi s}{H}\right) \right] & 0 < s \leq 2H \\ 0 & s > 2H \end{cases}, \quad (19)$$

where s represents the distance penetrated into the gust, H is the gust gradient, between 9 m and 107 m, U_{ds} is the gust velocity in equivalent airspeed,

$$U_{ds} = U_{\text{ref}} F_g \left(\frac{H}{107} \right)^{\frac{1}{6}}. \quad (20)$$

U_{ref} represents the reference gust velocity in equivalent airspeed, indicated by CS 25 regulation as a function of altitude for a gust gradient H of 107 m. Finally, F_g represents the flight profile alleviation factor and is minimum at sea level, linearly increasing to 1 at the certified maximum altitude.

The "1 – cos" model is simple and particularly useful to simulate large loads acting on the wing surface. However, to represent continuous and irregular nature of the atmospheric turbulence, a continuous gust model, based on von Kármán turbulence model, is proposed. This model defines the linear and angular velocity components of the continuous gust as a stochastic process and specify the Power Spectral Density (PSD) of each component by means of mathematical expressions [8]. For example, the power spectral density of the gust vertical component w_g is expressed as

$$\Phi_w(\omega) = \frac{2\sigma_w^2 L_w}{\pi V} \cdot \frac{1 + \frac{8}{3} \left(2.678 L_w \frac{\omega}{V} \right)^2}{\left[1 + \left(2.678 L_w \frac{\omega}{V} \right)^2 \right]^{\frac{11}{6}}}, \quad (21)$$

where V is the aircraft speed, σ_w defines the turbulence intensity, which is the Root Mean Square (RMS) gust component, and L_w represents the turbulence scale length. Both turbulence intensity σ and scale length L values depend on altitude and flight conditions, as indicated in the design procedures reported on [9].

The gust velocity time history is obtained by passing a band limited white noise through a forming filter derived from the gust PSD [13]. This leads to an output signal with the same PSD of the chosen model, which can be used directly as wind disturbance inside the rigid equations of motions.

2.4. Sensor Models: Accelerometers

As already mentioned the FMSC contains also different sensor models. Three accelerometers on each half-wing, to measure the accelerations due to bending and torsion of the flexible structure, an inertial measurement unit (IMU) and a global positioning system (GPS).

Focusing on the accelerometers, the model is similar to an IMU one, where the acceleration calculated by the rigid model is corrected taking into account the position of the accelerometers. Bias and random noise are included. The accelerations are evaluated in the mid-chord position of selected stations along the wing span.

An electrical model of the accelerometers, reported in Figure 2, is also provided. This electrical model has as input the acceleration along z-axis $\ddot{\xi}$ in which the flexibility of the aircraft is taken into account and has as output the voltage v . The voltage is evaluated according to

the sensor technical specifications. The sensitivity block converts the acceleration in to voltage, and takes as input also the temperature T , as the external temperature affects the sensitivity of the sensor. Then the obtained voltage is filtered by a low pass filter, since the sensitivity is also affected by the frequency of the input signal. The residual noise is modelled as bias, so a constant value v_0 is added to the voltage v , representing the voltage given in output when the acceleration in input is null. Finally, a saturation block simulates the limit tension values.

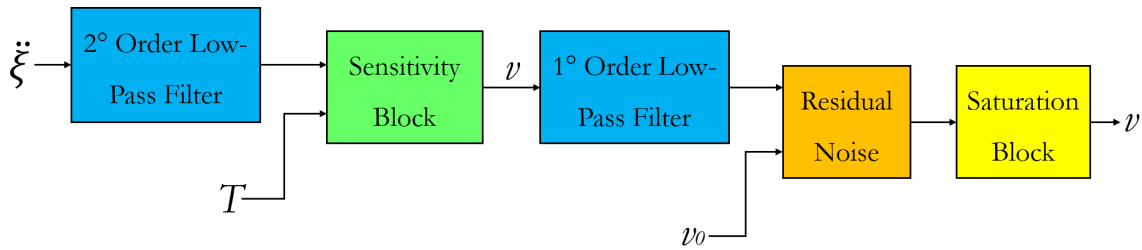


Figure 2. Electrical Model of the Accelerometers

2.5. Hinge Moments

The hinge moments, acting on control surfaces, takes as input the aircraft velocity, control surfaces deflections and air density and returns the hinge moments acting the respective control surface as output.

The hinge moment is calculated as the aerodynamic torque generated on the hinge axis by the variation of the pressure distribution acting on the control surfaces. Taking the aileron as example, its hinge moment can be simply evaluated as $H_a = \frac{1}{2}\rho V^2 S_a c_a C_{H_a}$, in which S_a represents the aileron surface and c_a represents the root chord of the aileron. C_{H_a} represents the respective hinge moment coefficient, which depends on the control surface geometry and its aerodynamic characteristics, and can be evaluated as follows [10]: $C_{H_a} = C_{H_0} + C_{H_\alpha} \alpha + C_{H_{\delta_a}} \delta_a$. The coefficients C_{H_0} , C_{H_α} and $C_{H_{\delta_a}}$ are evaluated from the control surface geometry. Particularly, the geometric parameters used in the coefficients evaluation are: the flap chord ratio ($\frac{c_f}{c}$), the airfoil thickness ratio ($\frac{t}{c}$) and the airfoil bevel angle (τ).

3. Simulation Results

In order to analyse the generic flexible wing response to a gust perturbation, the model described in Section 2.2 is implemented using Matlab/Simulink.

The model considers the aircraft in cruise phase at Mach 0.3 and 6000m , with an OEW (Operative Empty Weight) mass configuration (20147 kg).

The first analysed perturbation is a "1 – cos" vertical discrete gust as described in Eq. (19) with

$$H = 26 \text{ m} \quad U_{ref} = 17.07 \frac{\text{m}}{\text{s}}$$

The obtained gust profile is shown in Figure 3. This gust velocity is then used to describe the perturbation in terms of angle of attack $\alpha_g \approx \frac{wg}{V}$, which is in turn used in the rigid dynamics equations to perturb the aircraft $\alpha_{AC} = \alpha_{RIG} + \alpha_g$. The graphs in Figure 4 shows the wing response in terms of bending accelerations, measured by each one of the three wing accelerometers.

Another analysed perturbation consists in a von Kármán continuous vertical gust shown in Figure 5. The turbulence intensity σ_w (RMS) is set to "moderate" while the other parameters

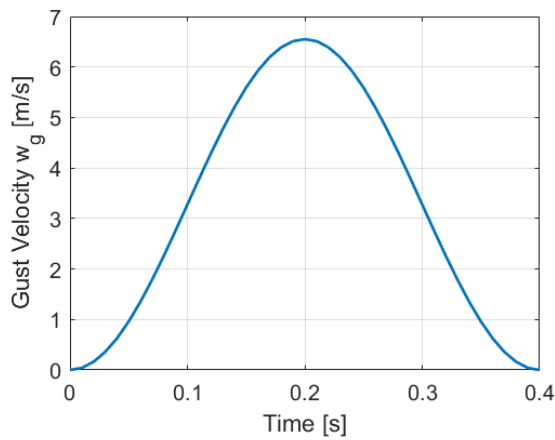


Figure 3. "1 – cos" Gust Profile

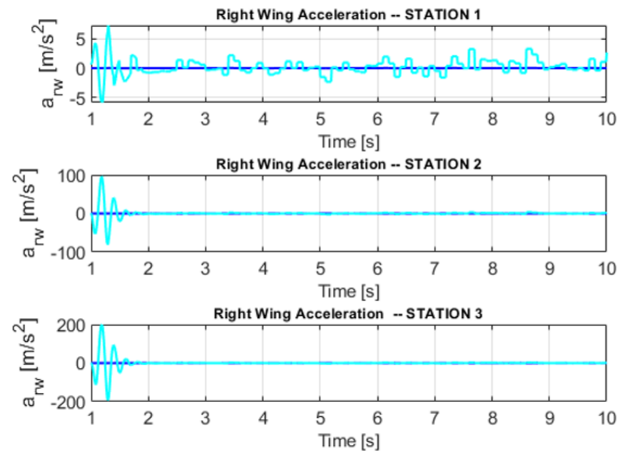


Figure 4. Bending Accelerations (discrete)

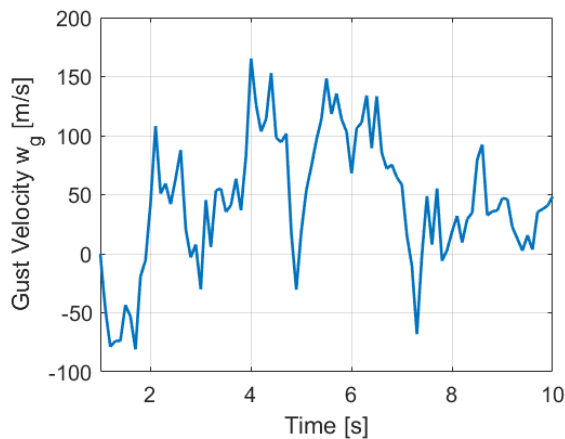


Figure 5. von Kármán Gust Profile

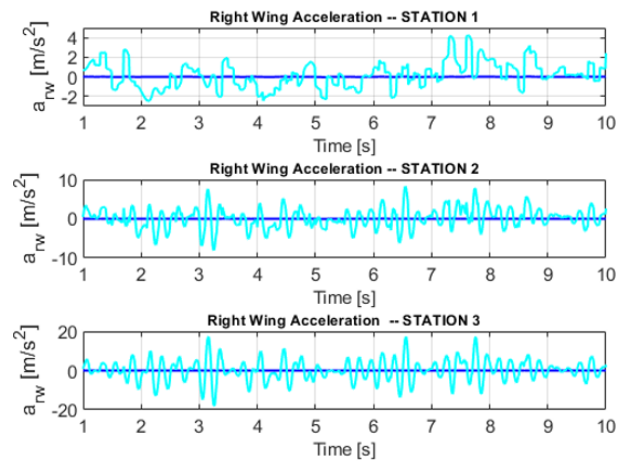


Figure 6. Bending Accelerations (von Kármán)

used in Eq. (21) are set accordingly to the procedures indicated in [8, 9, 13]. The wing response is in terms of flexible accelerations measured by the wing accelerometers, as shown in Figure 6.

Comparing the obtained results, the irregular nature of the wing response is immediately visible after a continuous randomly generated gust, especially when compared to the discrete gust response, which shows a typical second order dynamic system trend. In general, continuous gusts are used to excite the various elastic modes, while discrete gusts are used to generate and study large loads on the structure.

Lastly, also the hinge moments of each one of the control surfaces can be evaluated. Figure 8 shows as example the aileron hinge moment after the discrete gust reported in Figure 7.

4. Conclusions

As stated before, the described flexible model is a combination of Newton and Lagrange approaches, for a computational efficient algorithm, to be easily implemented for real-time simulations. In detail, the obtained set of equations is written by means of generalized coordinates using the Galèrkin method, reducing the complexity of the formulation and thus the computational load. Furthermore, the external aerodynamic forces can be expressed by means of the Rayleigh dissipation function. Since a strong link is maintained between rigid and

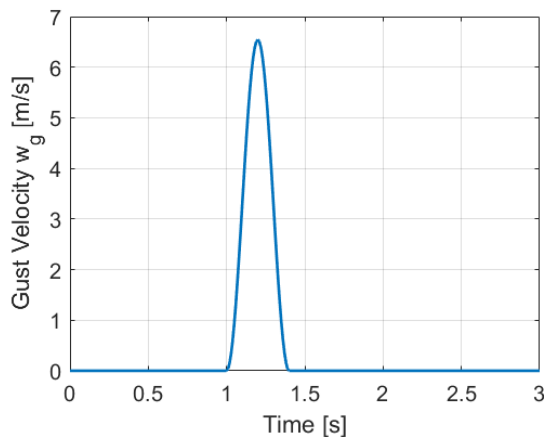


Figure 7. "1 – cos" Gust Profile

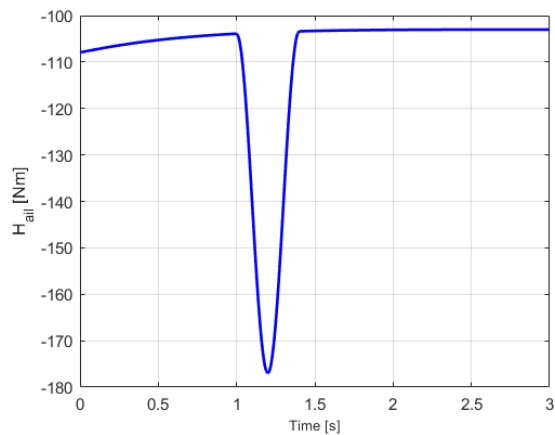


Figure 8. Aileron Hinge Moment (discrete)

flexible aircraft models, the flexible wing response to a gust can be evaluated by implementing the turbulence models directly as wind perturbation inside the rigid dynamics model. This is possible since both the presented discrete and continuous models express the gust as a wind velocity component. In this work, only vertical gusts are considered, as variation of the angle of attack. Finally, accelerometers on wing sections and hing moments are also included in the mathematical model. Numerical results demonstrate how the approach correctly represents flexibility effects on aircraft response for a transport aircraft model, even if a reduced number of modes is considered. Future works will include accurate structural data, from FEM analyses, to consider shape functions of high order modes in the model. Moreover, extensive simulations will be performed to better validate the model simplifications.

References

- [1] S. Song, J. F. Whidborne, M. Lone, and A. Molina-Cristobal, "Multi-objective optimal longitudinal flight control system design for large flexible transport aircraft," in *2018 UKACC 12th International Conference on Control (CONTROL)*, pp. 81–86, 2018.
- [2] C.-S. Chang, D. H. Hodges, and M. J. Patil, "Flight Dynamics of Highly Flexible Aircraft," *Journal of Aircraft*, vol. 45, pp. 538–545, Mar. 2008.
- [3] J. L. Junkins and Y. Kim, *Introduction to dynamics and control of flexible structures*. AIAA education series, Washington, D.C: American Institute of Aeronautics and Astronautics, 1993.
- [4] E. H. Dowell, *A Modern Course in Aeroelasticity*. Cham: Springer International Publishing, 2015.
- [5] R. Milne, *Dynamics of the Deformable Aeroplane*. Queen Mary College, London: Her Majesty's Stationery Office Reports and Memoranda Rept. 3345, 1964.
- [6] L. Meirovitch and I. Tuzcu, "Unified Theory for the Dynamics and Control of Maneuvering Flexible Aircraft," *AIAA Journal*, vol. 42, pp. 714–727, Apr. 2004.
- [7] G. Avanzini, E. Capello, and I. A. Piacenza, "Mixed Newtonian–Lagrangian Approach for the Analysis of Flexible Aircraft Dynamics," *Journal of Aircraft*, vol. 51, pp. 1410–1421, Sept. 2014.
- [8] F. M. Hoblit, *Gust loads on aircraft: concepts and applications*. AIAA education series, Washington, D.C: American Institute of Aeronautics and Astronautics, 1988.
- [9] U. S. Department of Defense, "Flying Qualities of Piloted Aircraft - U.S. Military Handbook MIL-HDBK-1797," Dec. 1997.
- [10] B. Etkin, *Dynamics of atmospheric flight*. Mineola, N.Y.: Dover Publications, 2005.
- [11] L. Meirovitch, *Principles and techniques of vibrations*. Upper Saddle River, N.J: Prentice Hall, 1997.
- [12] EASA, "Certification specifications and acceptable means of compliance for large aeroplanes cs-25, european aviation safety agency," 2015.
- [13] MATLAB Aerospace Blockset Documentations, *Von Karman Wind Turbulence Model (Continuous)*. Natick, Massachusetts: The MathWorks, Inc., 2019. Available on: <https://it.mathworks.com/help/aeroblks/vonkarmanwindturbulencemodelcontinuous.html>.